

FINITE ELEMENT ANALYSIS ON THE FORMATION OF RESIDUAL STRESSES DURING WELDING OF OIL AND GAS PIPE

MAHMOODALHAFADHI, GYORGY KRALLICS & MÁTÉ SZÜCS

Institute of Physical Metallurgy,

Metal Forming and Nanotechnology, University of Miskolc, Miskolc, Hungary

ABSTRACT

This study deals with the prediction of residual stress in oil and gas pipe welds using finite element (FE) method. Arc welding is widely used in industries such as piping, oil and gas pipeline, power plant station, etc. Non-uniform distribution of plastic and thermal strain is responsible for producing a large amount of residual stress and deformation in all welded structures, including pipelines. Numerical simulation can be used to predict residual stress in pipe welds; the aim of this paper is to find whether two-dimensional (2D) computations can be substituted for three-dimensional (3D) simulations. 2D asymmetric and 3D numerical simulations were used to predict the distribution of residual stress in arc welded pipes. In the FE simulation Goldak's ellipsoidal model is used to describe the moving heat source in each weld path. The effects of weld parameters on residual stress were investigated. The effects of welding power on residual stress and temperature fields at different locations were evaluated. Stresses in both the inner and outer walls of pipes were calculated by FEM. The results show that the 2D axisymmetric model can be effectively used to analyze and simulate the residual stress for steel pipe through the pipe thickness.

KEYWORDS: *Finite Element Analysis; Pipe Welding & Residual Stress*

Received: May 17, 2018; **Accepted:** Jun 07, 2018; **Published:** Jun 15, 2018; **Paper Id.:** IJMMSEAUG20181

1. INTRODUCTION

Pipelines which are known to be the arteries of industry and through these arteries fluids, vapor, gases, and solids flow in the direction of the condition imposed by the ongoing processes. These are sometimes subjected to the intense stresses caused by parameters such as temperature, pressure and flow and combinations of these processes, to the damages caused by corrosion, erosion, and explosion, to toxic conditions, residual stress and to diverse problems involving hygiene, heat and cold losses, handling of acids and alkalis. Until many years, the industries and the governments of various countries have increasingly shown their concern about the safety of pipes or protection of the pipelines. Sometimes the transportation of natural gas or crude oil has to be continuous for a long distance example for thousands of miles across the countries, which is only possible by pipelines (Ernest Holmes et.al.1973)[1]. Welding is a reliable and efficient metal joining process and used in almost all industries. Welded joints are extensively used in the fabrication industry, oil and gas pipe, offshore structures and pressure vessels. Steel pipes have been in common use for the engineering applications such as power plants, underground pipelines, etc. However, one of the major problems in welded structures is the welding residual stress, which can lead to cracking, fatigue, and even pipe failure. It is possible to determine the internal residual stresses in welded joints with experimental measurement as well as numerical simulation (Obeid et al., 2018) [2]. Because the experimental methods need special equipment and a long period to be executed, simulation results

have been reported based on the thermal elastic-plastic analysis by using finite element codes. Residual stress measurement has been mainly carried out by the Hole Drilling Method (Van Puymbroeck et al., 2018) [3], Cutting Method (Yong Suna et al., 2016)[4], and X-ray Diffraction Method. Residual stresses through the thickness direction at a specified position can be calculated by the finite element method (FEM). One research team (Woo et al., 2013; 2011) [5-6] reported that neutron can penetrate a 70 mm-thick weld plate. They also determined the residual stress distributions through the thickness of the welded steel plate. In the last studies, the finite element method has been presented to analyse and predict the residual stress that it is necessary to continue to compare the experimental result with numerical analysis. In addition, the three-dimensional and two dimensional models can be used to analysis residual stress in the model. Many authors have also proposed FEM models to predict residual stresses. It is good to compare the simulation analysis result of the 3D with the results of the 2D axisymmetric, that mean that a large amount of time can be saved if the 3-D model can be replaced by a 2-D axisymmetric. Goldack et al. [7] introduced a double ellipsoidal heat distribution model. Many others have also proposed FEM models to predict residual stresses. Deng and Murakawa [8] analyzed the temperature and residual stresses in multi-pass girth welds with SUS304 stainless steel pipe sections in 3-D and 2-D FE models. Their results of both 3-D model and 2-D obtained from ABAQUS are in very good agreement with experimental measurements. Jiang et al. [9] developed a sequential coupling finite element procedure to predict residual stresses and deformations in the butt welding of an ultra-thick tube-sheet in a large scale reactor by finite element method. ShugenXu et al. [10] employed FEM to predict the welding residual stresses in a layered-to-layered joint. An axisymmetrical thermal and mechanical model was established and validated by the experimental data. The results of numerical calculation show that large residual stresses are generated in both the weld and the Heat Affect Zone (HAZ). Teng and Chang [11] studied predicting the state of thermo-mechanical model behavior using FEM. Residual stresses were investigated in a three-dimensional FEM analysis of welded pipes. The influence of pipe thickness on residual stresses is also discussed. It was found that the thicker walled pipes have higher residual stresses than the thinner walled pipes. Friedman [12] employed the FE method to calculate temperatures, stresses and distortions during welding. Residual stresses were greatest in the weld metal and heat-affected zones. Yaghi et al. [13] presented the residual stresses in welded components and discussed a brief review of weld simulation FEM used for welded sections of steel pipes. Residual stresses in different directions were discussed with different thicknesses of 7.1 or 40.0 mm. Murugan et al. [14] employed a finite element model to compare the residual stress fields during welding with experimental work. X- ray diffraction was used to determine the residual stresses with different thickness of plate. The measurement method was used to validate finite element simulations of residual stresses in a welded pipe. There is good agreement between the predicted and measured distributions of residual stress. Smith et al. [15] examined the residual stress levels in a 50 mm thick ferritic steel submerged-arc weld using two destructive methods, the hole-drilling method and the block removal and layering method. The maximum residual stress was in the direction of weld. Jiang et al.[16] studied the residual stress in the range of 50 mm–100 mm thick plates by using FEM and the ND measurement, and they found both the heat input and plate thickness have little influence on the residual stress distribution. Lindgren et al. [17] used FEM (2D model) to simulate the welding residual stress in a 200 mm thick welded plate and the FEM results were compared with the experimental by the hole-drilling method. It is shown that both techniques give the same results. Mitra et al. [18] employed the finite element analysis to simulate the residual stress distributions in 800 mm thick joints produced by the narrow gap submerged arc welding, and the simulated results were verified with the X-ray diffraction (XRD) measurement. Yaghi et al. [19] explained the influence of residual stress using FE simulation thermal analysis and structural analysis in two welded halves of pipe with nickel-based alloy (IN625). Malik et al. [20] studied the

residual stress fields in circumferentially arc welded thin-walled cylinders. Ueda and Yamakawa [21] employed 2D finite element analysis to analyze the effect of geometry configuration on residual stress and compared the results with experimental values. Owen et al. [22] compared results from neutron diffraction, X-ray diffraction, synchrotron X-ray diffraction and FEM of residual stress developed during welding of aluminum alloy AA2024. Deng et al. [23] developed a 3D FE model for simulating residual stresses during multi pass welding of a pipe. The aim of this study is to investigate whether 2D analysis is appropriate for predicting residual stress in pipe welds.

2. MATERIALS AND METHOD

Physical Modeling

A pipe with outer diameter of 114.4 mm, thickness of 6 mm, and a total length of 400 mm was considered for the analysis shown in Figure 1b. The welding begins at the central angle ($\theta=0^\circ$) and in clockwise direction. As shown in Figure 1d, each weld bead started and ended at 0° location. Figure 1a shows the 3-D finite element model using MSC Marc. In this model, the number of elements is 13440. Since this material is widely used in engineering pipe, the material used is steel. The material X5CrNiMo18 dimension, arc welding with two passes and the filler material is also same steel used in this work presented by Dean Deng et. al [8]. This material was selected because most of the previous studies were about austenitic steels in this work, phase transformation is neglected. The welding conditions for the two passes are shown in Table 2.

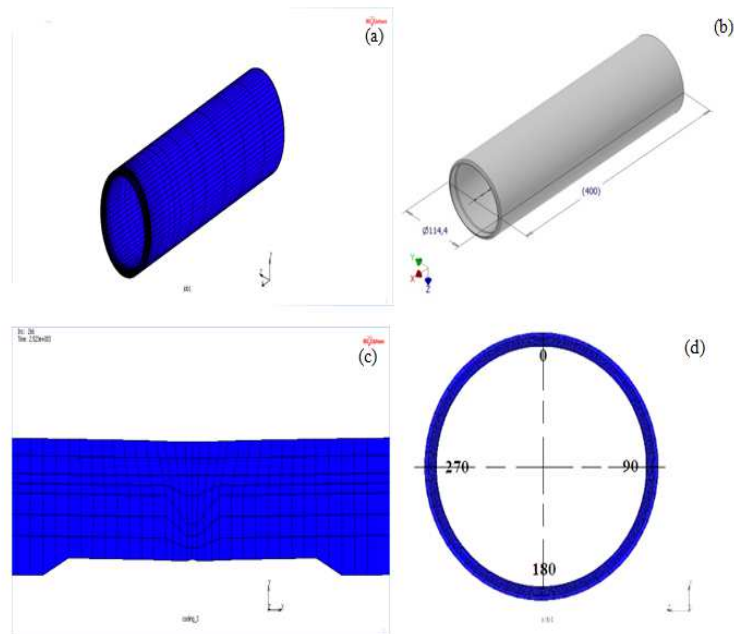


Figure 1: (a) 3-D Finite Element Model of Pipe (b) Dimensions of Pipe (c) 2-D Finite Element Model (d) Welding Direction

Table 1: Welding Parameters [25]

Pass number	Current	Voltage	Speed	Weld Pool Parameters		
	(A)	(V)	m/min	a (mm)	b (mm)	$c_r c_r$ (mm)
1	140	9.5	80	4	3	5,8
2	160	9.5	80	4	3	5,8

2-D finite element model and weld passes are shown in Figure 2a. In this model with filler, the number of nodes is

520, and the number of elements 450. Figure 2b shows the dimensions of analysis model. The results of the temperature fields and the residual stress distribution suggest that it is feasible to conduct the thermal analysis and the mechanical analysis for the X5CrNi18 pipe using a 2-D axisymmetric model. In the thermal analysis, a volumetric heat source with uniform density is employed. The computational procedure used in the 2-D model (figure 1c) is the same as the 3-D model.

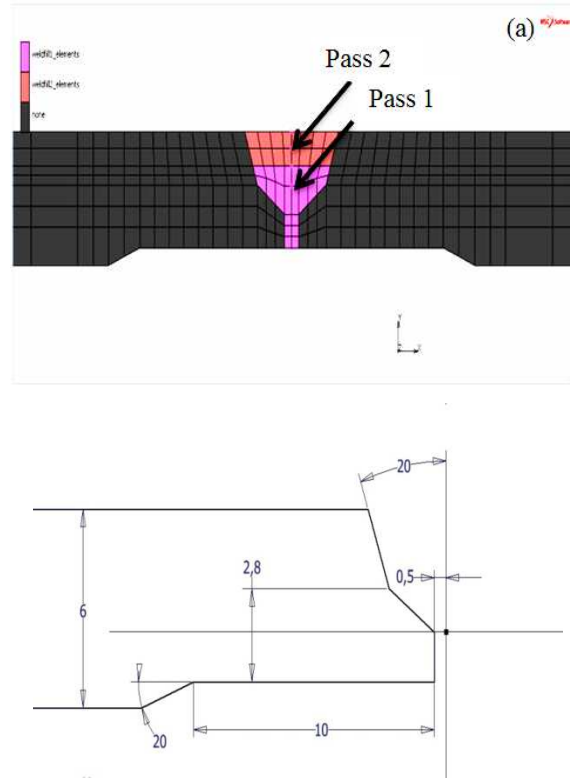


Figure 2: (A) 2D Asymmetric Model with Fillers (B) Dimensions of Analysis Model.
(All Dimensions are in Mm)

2. Welding Thermal Process with Specialized Boundary Conditions

The model that was used is based on a double ellipsoidal heat source model distribution presented by Goldak et al. (1984, 1986). The distribution has the capability of analyzing the thermal history (thermal distribution over time) of a deep penetration weld. The distribution of this model when expressed in moving Cartesian coordinate system (x, y, and z) is expressed by equations:

Distribution inside the front quadrant:

$$Q_f(x, y, z) = \frac{6\sqrt{3}f_f\eta VI}{abc\pi\sqrt{\pi}} \exp\left(\frac{-3x^2}{a^2}\right) \exp\left(\frac{-3y^2}{b^2}\right) \exp\left(\frac{-3z^2}{c^2}\right) \quad (1)$$

Similarly, for the rear quadrant:

$$Q_r(x, y, z) = \frac{6\sqrt{3}f_r\eta VI}{abc\pi\sqrt{\pi}} \exp\left(\frac{-3x^2}{a^2}\right) \exp\left(\frac{-3y^2}{b^2}\right) \exp\left(\frac{-3z^2}{c^2}\right) \quad (2)$$

Where Q_f and Q_r are the weld flux rates per unit volume in the front and rear weld pools respectively; $Q = \eta VI$ is the applied power. It is the product of the arc voltage (V), welding current (I), and process efficiency (η). The efficiency of arc η , is assumed to be 70% for the welding process ; a is the weld width along the tangent direction x; b is the weld

penetration depth along the arc direction y; c_f and c_r are the forward and rear weld pool lengths in the weld path direction z; and are dimensionless factors given by

$$f_f = \frac{2}{(1+c_f/c_r)} \quad (3)$$

$$f_r = \frac{2}{(1+c_f/c_r)} \quad (4)$$

The pipe geometry is generated and welding torch is applied along the circumference using the welding parameters given in Table 1. The pool welding parameters and the double ellipsoidal source are also shown in Figure3.

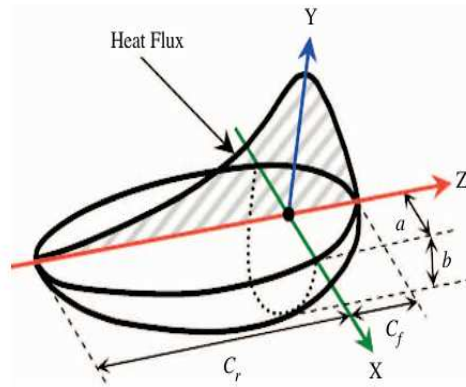


Figure 3: Double Ellipsoid Heat Source

3D finite element model was developed. In this study, all analyses are performed using Mac Marc code [24]. The base metal and weld metal are defined as the same materials. The thermal properties and mechanical properties of the metal are shown in Table 2.

Table 2: Thermal Physical Properties and Mechanical Properties of X5crnimo18 [8]

Temperature (°C)	Density (g/mm ³)	Yield stress (MPa)	Young's modulus (GPa)	Poisson's ratio
0	0.79	265	198.5	0.294
100	0.788	218	193	0.295
200	0.783	186	185	0.301
300	0.779	170	176	0.31
400	0.775	155	167	0.318
600	0.766	149	159	0.326
800	0.756	91	151	0.333
1200	0.737	25	60	0.339
1300	0.732	21	20	0.342
1500	0.732	10	10	0.388

FEM thermal Analysis is employed with same finite element mesh here. The mechanical analysis is conducted using the temperature histories computed by the thermal analysis as the input data. Mechanical analysis is used to fix model motion. Because of the symmetry of the model, in 3D and 2D axisymmetric models, the symmetry plane is fixed in Y-direction. The three components needed to calculate the total strain rate can be written as:

$$\dot{\epsilon} = \dot{\epsilon}^e + \dot{\epsilon}^p + \dot{\epsilon}^{th} \quad (5)$$

where ϵ^e is the elastic strain, ϵ^p is the plastic strain and ϵ^{th} is the thermal strain. The high temperature values in the

surfaces lead to non-uniform plastic deformation in around the weld zone. Residual stress is induced by welding occurs due to non-uniform heating and cooling phases. Generally, some shrinkage and deformation occurs in welding of pipes because of variable cooling rates in different regions in the weld zone. [29]

3. RESULTS AND DISCUSSIONS

Numerical Summation of 3-D Model

Results are presented here for residual stress analysis in the pipe showing the axial and hoop with different surfaces. It is also shown for the effect of power sources and pipe thickness on residual stress.

Figure 4 shows the axial stress on the welded pipe. The axial stresses at the start of welding and in its vicinity are slightly different from the other locations. Figure 5 shows temperature distribution during welding and start / stop at same point of the welding.

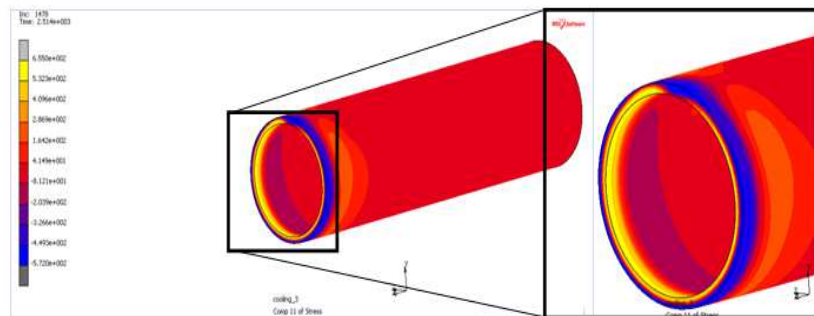


Figure 4: Axial Stress Distributions Around The Welded Lined Pipe.

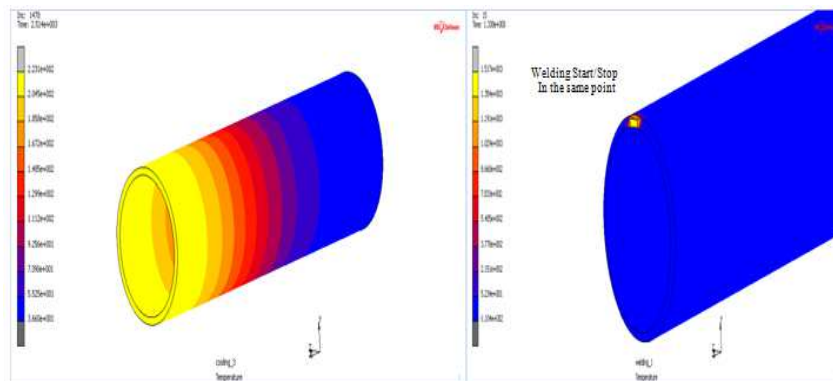


Figure 5: Predicted Temperature Distribution During Welding

Figure 6 shows the axial stresses and the hoop stress at locations with different angle θ . Figure 6a shows axial stress distributions on the inside surface, while Figure 6b shows hoop stress distribution. When θ is 0° the hoop stress distribution in weld zone and its vicinity is slightly different from that of other three locations ($\theta = 90^\circ$, 180° and 270°) because of the end effect. When θ is 90° the hoop stress at locations $X = 30$ mm is the smaller than that of the other three locations ($\theta = 0^\circ$, 180° and 270°). However, neither the axial stress nor the hoop stress is significantly sensitive to the angle. The 2-D axisymmetric model is used to compare the simulation results of the 3-D. In order to reduce the computational time most researchers choose the 2D axisymmetric models. The 2-D model not only can save a large time

for computing but also can accurately predict the residual stress in pipe welding.

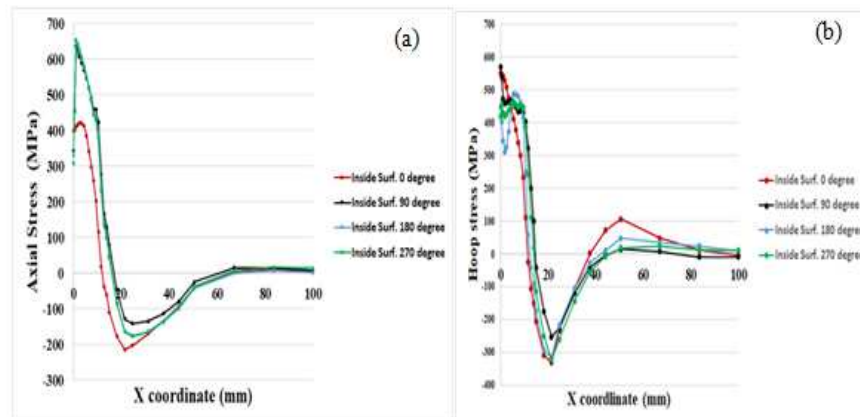


Figure 6: Distributions on the Inner Surface (A) Axial Stress (B) Hoop Stress.

Figure 7 shows the axial stress and hoop distribution of the welded pipe at the outer surface of pipe at different orientations of 0°, 90°, 180° and 270° from weld start point.

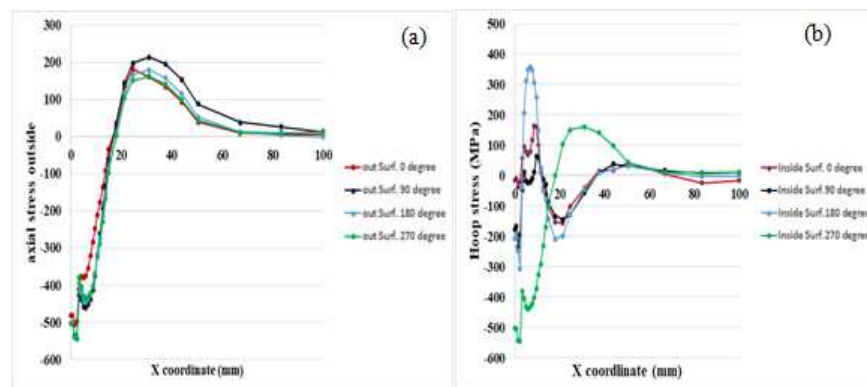


Figure 7: Distributions on the Outer Surface (A) Axial Stress (B) Hoop Stress

Figure 7a shows the axial stress distribution at the outside surface for different angles of pipe. From the figure it can be seen that at the weld pool the nature of residual stress is compressive, and then it gradually decreases and after a distance of 40 mm from weld center line its nature changes to tensile, turning to a positive maximum. At a distance of 55 mm from the weld line, the stress has a value close to zero, i.e. at a distance of about 60-80 mm the residual stress has no influence and has a very low value. The maximum value of the tensile stress is about 210 MPa and the same in the compressive region is about 550 MPa. From the figure it can also be observed that the stress variation at the weld start position (at 0° orientation) is slightly different than the other positions.

From Figure 7b it can be seen that in almost all positions the stress pattern is different. Stress comes to a negative maximum of 550 MPa and finally at a distance of 60 mm from the weld centerline the residual stress vanishes. The maximum stress value in the tensile region is about 350 MPa.

Comparison of 3D With 2D

Figure 9 shows the 3D finite element simulation results compared with 2D results. Axial stress at 0° shows good agreement especially inner surface and outer surface because this good agreement, in later numerical computation

the 2D data is used in order to save computation time. It is absorbed that is the 2D result similarly with 3D. The purpose of numerical analyses in 2D axisymmetric to investigate the influence of residual stress through the thickness of the pipe.

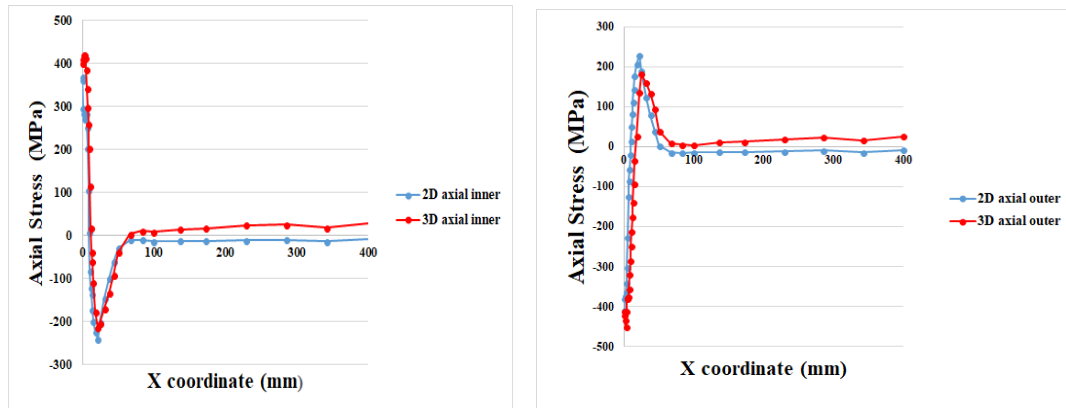
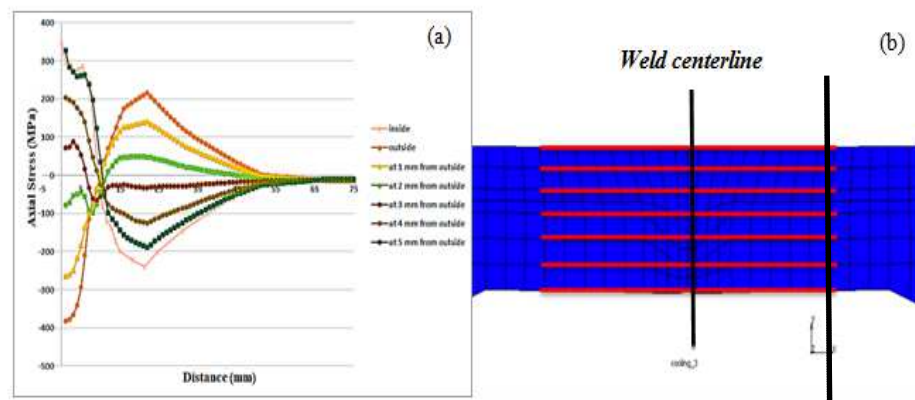


Figure 9: Comparison of the 3D with the 2D

Residual Stress through the Thickness of Pipe

The axial stress variations at different depths through the thickness of pipe are as shown in Figure 10 from the figure, it is clear that from the weld centerline, the residual stress changes in nature. Around 10 mm from the center line, the stress is tensile and compressive. On the outer surface we can observe that maximum value of compressive stress is found at the centerline. However, Farther from the weld the value switches to tensile stress, reaching 200 MPa. The opposite occurs for the stress value of the inner surface. Further it can be seen that at a distance of 3 and 4 mm from the outer surface of pipe, the value of residual stress is very low compared to all other depths. This result suggests that there is a lines where the residual stress has negligible effect, i.e., there exists a line of zero stress in the middle layer of the pipe. The results show very similar trend to the 3D simulation results of Prasad et al. [25].



**Figure 10: (A) Variation of Residual Stress along Length of Pipe through Thickness
(B) The Welding Centerline**

4. CONCLUSIONS

The finite element method is used to determine the residual stress field during and after welding. High compressive stress develops on the outer surface and a tensile residual stress develops on the inner surface.

From the outer surface to inner surface the nature of residual stress changes from compressive to tensile. The main results are summarized as follows:

In the present study, both the 3-D FE model and the 2-D axisymmetric FE model predicted welding residual stress fields. The three-dimensional numerical analysis of welding requires a large memory and time. Temperature and residual stress distributions were analyzed, 2-D axisymmetric can be saved the time and numerical analysis.

2-D asymmetric model and 3D both are good agreement.

Stresses in both the inner and outer walls of pipes were calculated by FEM.

From the simulated finite element model, the temperature distribution and residual stress distribution can be obtained.

Steady temperature distributions are obtained after the welding source passes.

Residual stress changes from compressive to tensile from outer to inner surface after the welding along and near the weld line.

ACKNOWLEDGMENT

The Authors Are Thankful To Csabapuskas For Help Us

REFERENCES

1. Ernest Holmes, *Handbook of industrial pipework engineering*, McGraw-Hill Book Company (UK) Limited, (1973), pp.3-4.
2. Obeid Obeid, Giulio Alfano, Hamid Bahai and Hussam Jouhara, *Numerical simulation of thermal and residual stress fields induced by lined pipe welding*, *Thermal Science and Engineering Progress Volume 5*, March (2018), pp. 1-14.
3. Evy Van Puymbroecka, Wim Nagya, Heng Fanga, Hans De Backe, *Determination of residual weld stresses with the incremental hole-drilling method in tubular steel bridge joint*, *Procedia Engineering*, (2018), pp. 651–661.
4. Yong Suna, Vladimir Luzin, William J.T. Daniel, Paul A. Meehan, Mingxin, Zhang Shichao Dinga, *Development of the slope cutting method for determining the residual stresses in roll formed products*, *Measurement Volume 100*, 2017, pp. 26-35.
5. W. Woo, G.B. An, E.J. Kingston, A.T. DeWald, D.J. Smith, M.R. Hill *Through-thickness distributions of residual stresses in two extreme heat-input thick welds: a neutron diffraction, contour method and deep hole drilling study* *Acta Mater.*, 61, (2013), pp. 3564-3574.
6. W. Woo, V. Em, P. Mikula, G.B. An, B.S. Seong, *Neutron diffraction measurements of residual stresses in a 50 mm thick weld* *Mater. Sci. Eng. A*, 528 (2011), pp. 4120-4124.
7. John Goldack, Aditya Chakravarti and Malcolm Bibby., *A new finite element model for welding heat sources*, *J. Metallurgical Transactions B* 15, (1984), pp. 299-305.
8. Dean Deng, Hidekazu Murakawa, *Numerical simulation of temperature field and residual stress in multi-pass welds in stainless steel pipe and comparison with experimental measurements*, *Journal of Computational Materials Science* 37, (2006), pp. 269 – 277.
9. Jian LIN, Ninshu MA, Yongping LEI and Hidekazu MURAKAWA. *Measurement of Residual Stress in Arc Welded Lap Joints by $\cos\alpha$ X-ray Diffraction Method*. *Journal of Materials Processing Technology*.

10. Shugen Xu, Yanling Zhao, Numerical investigation on weld residual stresses in tube to tube- sheet joint of a heat exchanger. *International Journal of Pressure Vessels and Piping* 101, (2013), pp.37-44.
11. T. Teng, P. Chang .Three-dimensional thermomechanical analysis of circumferentially welded thin-walled pipes .*Int J Press Vess Piping*, 75, (1998), pp. 237-247.
12. E. Friedman Thermomechanical analysis of the welding process using the finite element method *J Press Vess Technol*, 97, (1975), pp. 206-213.
13. Adewoye, Jonathan Oyerinde, and C. O. Olaoye. "Usage of information technology to enhance professional Productivity among accountants in Ekiti State." *International Journal of Accounting and Financial Management Research (IJAFMR)*4.2 (2014): 7-18.
14. A.H. Yaghi a, T.H. Hyde b, A.A. Becker b and W Sun. Finite element simulation of residual stresses induced by the dissimilar welding of a P92 steel pipe with weld metal IN625 *International Journal of Pressure Vessels and Piping* 111-112., (2013), pp.173-186.
15. S. Murugan, S.K. Rai, P.V. Kumar, T. Jayakumar, Baldev Raj, M.S.C. Bose .*International Journal of Pressure Vessels and Piping*, 78, (2001), pp. 307-317
16. D.J. Smith, P.J. Bouchard, D. George, Measurement and prediction of residual stresses in thick-section steel welds, *J. Strain Anal.*, 35 (4), (2000), pp. 287-305.
17. W. Jiang, W. Woo, Y. Wan, Y. Luo, X. Xie, Evaluation of through-thickness residual stresses by neutron diffraction and finite-element method in thick weld plates, *J. Press. Vessels Technol.*, 139, (2017).
18. L.E. Lindgren, H. Runnemalm, M.O. Näsström, Simulation of multipass welding of a thick plate, *Int. J. Numer. Methods Eng.*, 44, (1999), pp. 1301-1316.
19. A. Mitra, N.S. Prasad, G.D.J. Ram, Estimation of residual stresses in an 800 mm thick steel submerged arc weldment, *J. Mater. Process. Technol*, 229, (2016), pp. 181-190.
20. A.H. Yaghi, T.H. Hyde, A.A. Becher, W. Sun, Finite element simulation of residual stresses induced by the dissimilar welding of a P92 steel pipe with weld metal IN625, *Int. J. Press. Vessels Pip.* , 111–112, (2013), pp. 173-186.
21. Afzaal M. Malik, Ejaz M. Qureshi, Naeem Ullah Dar, Iqbal Khan, Analysis of circumferentially arc welded thin-walled cylinders to investigate the residual stress fields, *J. Thin-Walled Structures*-46, (2008), pp. 1391– 1401.
22. Y. Ueda, T. Yamakawa, Analysis of thermal elastic–plastic stress and strain during welding by finite element method *Trans. Jpn. Weld. Soc.*, 2 (2), (1971), pp. 90-100.
23. R.A Owen, R.V Preston, P.J Withers, H.R Shercliff, P.J Webster, Neutron and synchrotron measurements of residual strain in TIG welded aluminium alloy 2024, *Materials Science and Engineering: A* 346, 1–2, 15, (2003), pp.159-167.
24. D. Deng, S. Kiyoshima, K. Ogawa, N. Yanagida, K. Saito, Predicting welding residual stresses in a dissimilar metal girth welded pipe using 3D finite element model with a simplified heat source *Nucl. Eng. Des.*, 241 (1) (2011), pp. 46-54.
25. Marc® 2013 Volume A: Theory and User Information, pp. 270-272.
26. Varma Prasad V.M., Joy Varghese V.M., Suresh M.R., Siva Kumar D., 3D simulation of residual stress developed during TIG welding of stainless steel pipes, *Procedia Technology* 24 (2016), pp. 364 – 371.